AUTHOR QUERY FORM

ELSEVIER	Journal: ENGEO Article Number: 3563	Please e-mail or fax your responses and any corrections to: E-mail: Corrections.ESCH@elsevier.spitech.com Fax: +1 619 699 6721

Dear Author,

Please check your proof carefully and mark all corrections at the appropriate place in the proof (e.g., by using on-screen annotation in the PDF file) or compile them in a separate list. Note: if you opt to annotate the file with software other than Adobe Reader then please also highlight the appropriate place in the PDF file. To ensure fast publication of your paper please return your corrections within 48 hours.

For correction or revision of any artwork, please consult http://www.elsevier.com/artworkinstructions.

Any queries or remarks that have arisen during the processing of your manuscript are listed below and highlighted by flags in the proof. Click on the 'Q' link to go to the location in the proof.

Location in article	Query / Remark: click on the Q link to go Please insert your reply or correction at the corresponding line in the proof
Q1 OK, affiliation changed	Please confirm that given names and surnames have been identified correctly.
Q2 Revised, uploaded in separate file	Highlights should consist of only 85 characters per bullet point, including spaces. However, the Highlights provided for this item exceed the maximum requirement; thus, they were not captured. Kindly provide replacement Highlights that conform to the requirement for us to proceed. For more information, please see the Guide for Authors.
Q3 Yes, see proofs	Is the word "planforms" spelled correctly? Please check, and amend if necessary.
Q4 No, see proofs	Please note that Fig. 5 was not cited in the text. Please check that the citation suggested by the copyeditor is in the appropriate place, and correct if necessary.
Q5, Q6 See at the end of reference list	Citation "Papa et al. (2008)" has not been found in the reference list. Please supply full details for this reference.
Q7 See at the end of reference list	Citation "Cattoni et al. (2007)" has not been found in the reference list. Please supply full details for this reference.
Q8 CRC Press	Please supply the name of the publisher.
Q9 Paper was accepted and should be in press	Please provide an update for reference "Tarantino and El Mountassir, in press". Please check this box if you have no corrections to make to the PDF file. ☐

Thank you for your assistance.

Engineering Geology xxx (2013) xxx–xxx

Contents lists available at SciVerse ScienceDirect

Engineering Geology

journal homepage: www.elsevier.com/locate/enggeo

An approach for predicting the stability of vertical cuts in cohesionless soils above the water table

OK

Samuel A. Stanier [a], Alessandro Tarantino [b,*]

[a] Centre for Offshore Foundation Systems, The University of Western Australia, Australia
[b] ~~Department of Civil Engineering~~, University of Strathclyde, UK

Change

Department of Civil and Environmental Engineering

ARTICLE INFO

Article history:
Received 1 December 2011
Received in revised form 4 March 2013
Accepted 10 March 2013
Available online xxxx

Keywords:
Excavation
Laboratory tests
Limit analysis
Partial saturation
Shear strength
Suction

ABSTRACT

Temporary vertical excavations in cohesionless (granular) soils pose a problem for conventional 'two-phase' soil mechanics theory since non-zero collapse height is not predicted using the classical 'dry/saturated' shear strength criterion, given that cohesionless soils above the water table are assumed to be dry. An extension of the classical shear strength equation to account for the effect of matric suction on the effective stress in partially saturated soil is presented here that is incorporated into the bound theorems of plasticity. A simple validation experiment is reported to test the concept following which, a case study is presented that explores the extent to which matric suction and its impact on shear strength can explain the large safe vertical cut height that is often observed in cohesionless pozzolan deposits in the field. Lastly, the impact of rainfall events and subsequent ponded infiltration is investigated using a very simple analytical technique based on the classical Terzaghi consolidation solution. The research presented here gives practitioners with no particular expertise in the mechanics of unsaturated soil, techniques to assess the stability of geostructures involving unsaturated cohesionless soils that are based on simple calculation techniques taught in undergraduate courses.

1. Introduction

The stability of vertical excavations in cohesionless (granular) soils is an important problem in geotechnical engineering and engineering geology. Because excavations are typically carried out above the water table cohesionless soils are unsaturated. In routine geotechnical engineering and engineering geology calculations cohesionless soils (with no or little clay fraction) above the water table are generally assumed to be dry. Nonetheless this assumption is not accurate.

Soils above the water table, due to matric suction, are in fact partially saturated and also exhibit significantly higher shear strength than dry soils. As a result, vertical cuts up to several metres in height may remain stable (Tsidzi, 1997; Whenham et al., 2007; De Vita et al., 2008) in cohesionless soils. The beneficial effect of partial saturation is often exploited by contractors who typically cover the bank adjacent to the excavation with an impermeable membrane to divert surface runoff during heavy rainfall, thus preserving partial saturation. The beneficial effect of partial saturation on the stability of vertical and near-vertical cuts is recognised by engineering geologists when analysing and modelling bank retreat and delivery of bank sediments to river (Rinaldi and Casagli, 1999; Simon et al., 2000; Rinaldi et al., 2004). These mechanisms should potentially be incorporated into morphodynamic models of ~~the evolution river planforms~~ (Langendoen et al., 2012; Nardi et al., 2012). Partial saturation plays an important role in the stability of trenches (Vanapalli and Oh, 2012), which are used in a variety of applications in assessing geologic hazards in engineering geology, and tailing dams (Zandarín et al., 2009). The effect of partial saturation is also well known to children when erecting sand castles.

river-planform evolution

Change

Classical 'dry/saturated' soil mechanics fails to predict a non-zero safe vertical cut height in cohesionless soils above the water table, as they are assumed to be dry. In theory a dry cohesionless soil exhibits a zero collapse height, as is evidenced by the lower bound theorem of plasticity (Chen, 2007) or experimentally by observation, since it is impossible to fabricate a cylindrical sample of dry sand.

However, practitioners and academicians still find it convenient to disregard the contribution of partial saturation to shear strength as this leads to conservative design. This point of view can be questioned. Significant costs might be saved if 'new' geostructures are designed to account for the effects of partial saturation. Furthermore, geotechnical engineers and engineering geologists are often confronted with 'existing' stable yet potentially hazardous geostructures, e.g. steep slopes, for which conventional soil mechanics theory offers no explanation of the current state of equilibrium. In this case, a realistic analysis of the current state of stress is required, including characterisation of the partially saturated zone above the water table. This is essential when assessing the likelihood of future instability and hence, is a key to

* Corresponding author at: Department of Civil Engineering, University of Strathclyde, 107 Rottenrow, G4 0NG Glasgow, Scotland, UK. Tel.: +44 141 548 3539; fax: +44 141 553 2066.
E-mail address: alessandro.tarantino@strath.ac.uk (A. Tarantino).

0013-7952/$ – see front matter © 2013 Published by Elsevier B.V.
http://dx.doi.org/10.1016/j.enggeo.2013.03.012

ensuring the proposal of appropriate precautionary or remedial measures.

To quantify the effects of partial saturation on the stability of geostructures, methods should be developed to analyse collapse conditions in cohesionless partially saturated soils. So far, this problem has received little attention from researchers working on the mechanical behaviour of unsaturated soils.

This paper presents an approach based on the upper and lower bound theorems of plasticity. By assuming that the shear strength of partially saturated soils is controlled by the average skeleton stress, the classical approach developed for dry and saturated soils can easily be extended to cater for problems involving partially saturated soils.

Experimental evidence of the validity of this concept is provided in the form of collapse tests performed on cylindrical samples of partially saturated sand. Because changes in suction and vertical stress along the sample height are not negligible, this unconfined compression test is regarded as a boundary value problem rather than an element test. The theoretical analysis of the column collapse load based on the upper and lower bound theorems is thus essentially the same as the analysis that will be carried out to determine the collapse height of a vertical cut.

The principal goal of the paper is to verify whether the upper and lower bound collapse loads determined theoretically, bracket closely the values observed in the model tests. This is aimed at validating an approach to predict the collapse height of unsaturated cohesionless soils based on the bound theorems of plasticity.

A case study concerning the safe unsupported vertical cut height potentially achievable in pyroclastic silty sand (Pozzolan deposits) is then presented. This illustrates the utility of the proposed extension of the bound theorems of plasticity when assessing geotechnical and engineering geology problems in the field involving unsaturated soils.

2. Extension of the bound theorems of plasticity to unsaturated soils

The upper and lower bound theorems of plastic collapse set limits to the collapse load of a structure and can be proven for the case of perfectly plastic materials with associated flow rule (Chen, 2007). In two-phase soils, the failure (yield) criterion under ultimate conditions can be defined by the following equation:

$$\tau = (\sigma - u)\tan\phi' \tag{1}$$

where τ is the shear stress, σ is the normal stress, u is the pore pressure and ϕ' is the effective angle of shearing resistance. Pore pressure equals the pore-water pressure u_w in saturated soils and the pore-air pressure u_a in ideally dry soils. Using the failure criterion given by Eq. (1), the ultimate conditions of soil structures such as retaining walls, foundations, vertical cuts, and slopes can be assessed for saturated and dry soil (Atkinson, 1981; Chen, 2007).

The application of bound theorems of plasticity to soil structures above the water table requires the definition of a suitable failure criterion for partially saturated soils. For compacted (aggregated) soils, shear strength under partially saturated states can be expressed by the following equation (Tarantino and Tombolato, 2005):

$$\tau = (\sigma - u_w S_{re})\tan\phi' = (\sigma + sS_{re})\tan\phi' \tag{2}$$

where u_w is the pore-water pressure, s is the suction ($s = -u_w$), and S_{re} is an effective degree of saturation (degree of saturation of the macro-pores), which is given by:

$$S_{re} = \frac{e_w - e_{wm}}{e - e_{wm}} \tag{3}$$

where e is the void ratio (volume of voids per volume of solids), e_w is the water ratio (volume of water per volume of solids), and e_{wm} is the 'microstructural' water ratio, which separates the region of inter-aggregate porosity from the region of intra-aggregate porosity (Romero and Vaunat, 2000). The parameter e_{wm} may conveniently be determined by best fitting of shear strength data and the validity of Eq. (2) in conjunction with Eq. (3) has been proven by Tarantino (2007) and Tarantino and El Mountassir (in press) for a wide range of clayey soils, including compacted, and natural soils.

On the other hand, reconstituted and non-clayey soils are generally non-aggregated and the 'microstructural' water ratio e_{wm} may therefore be expected to be zero for these soils. Indeed, this has been demonstrated to be the case for a wide range of non-clayey soils by Tarantino and El Mountassir (in press).

For non-aggregated soils, the failure criterion can therefore be defined by the following equation (Öberg and Sällfors, 1997):

$$\tau = (\sigma - u_w S_r)\tan\phi' = (\sigma + sS_r)\tan\phi'. \tag{4}$$

If Eq. (2) or (4) is used in place of Eq. (1), collapse of geostructures in partially saturated soils can be analysed in a very similar manner by introducing a few simple modifications. To derive the upper bound solution, the work done by the internal stresses W_i for the case of translational failure can be written as (assuming an effective cohesion $c' = 0$):

$$W_i = \delta \sin\phi' \int_l sS_{re}\,dl \tag{5}$$

where δ is the magnitude of the block displacement, ϕ' is the effective (saturated) angle of shearing resistance, s is the suction, S_{re} is the effective degree of saturation, and l is the length of the failure surface. It is worth mentioning that the work done by the internal stresses W_i is written here in terms of total stresses whereas the external work associated with the gravitational load is calculated by considering the (total) soil unit weight.

To derive the lower bound solution, the failure criterion must not be exceeded at any point in the soil. This occurs if none of the Mohr's circles cross the failure envelope in the $\sigma + sS_{re}, \tau$ plane (rather than the σ', τ plane as in the case of saturated or dry soils).

3. Laboratory validation

3.1. Material

Experimental verification of the proposed extension to the bound theorems of plasticity was performed using a fine silica sand with grain size range of 0.075–0.2 mm and specific gravity, G_s, of 2.73 (derived experimentally). This material was expected to commence desaturation under applied suctions of less than 5–10 kPa, allowing a simple negative water column technique to be used to apply suctions to the base of a sample.

3.2. Water retention behaviour

3.2.1. Apparatus

To derive the water retention characteristics of the fine sand a simple negative water column method was employed. The apparatus used is shown schematically in Fig. 1. A cylindrical cell was used to house the sand sample and allow application of suction at the base. Different magnitudes of suction were applied to the sand sample by raising and lowering a water reservoir on a frame. A ThetaProbe sensor (Delta-T Devices Ltd., 1999) was placed in the sample at the surface to measure the volumetric water content at a known location. A high air-entry filter (with an air entry value greater than the maximum suction to be applied during the experimental procedure) was specifically devised to provide an interface between the sand and the hydraulic reservoir, thus maintaining suction.

Please cite this article as: Stanier, S.A., Tarantino, A., An approach for predicting the stability of vertical cuts in cohesionless soils above the water table, Engineering Geology (2013), http://dx.doi.org/10.1016/j.enggeo.2013.03.012

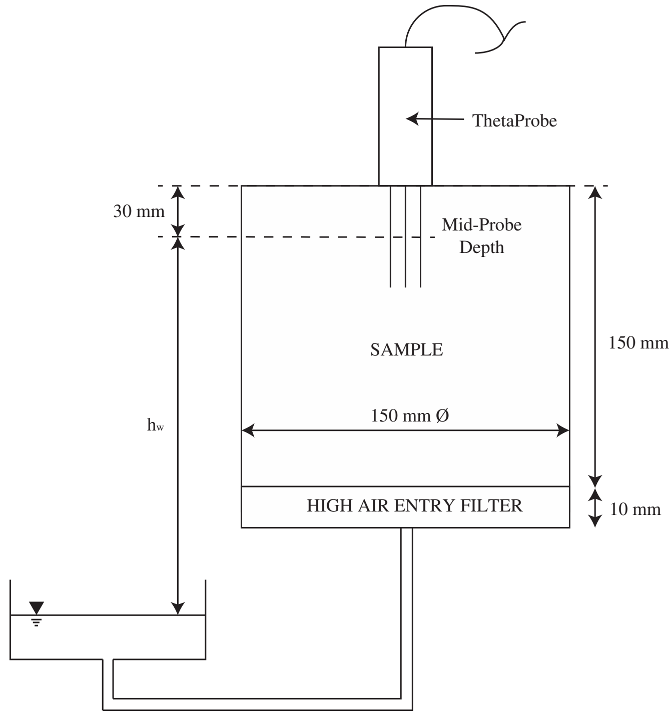

Fig. 1. Schematic of apparatus used to derive soil water retention behaviour of very fine uniform sand.

3.2.2. Sensor for water content measurement

The ThetaProbe sensor was used to measure the bulk dielectric permittivity of the soil, which is then correlated to the soil water content via calibration. The probe has a sensing length of 60 mm and the measurements taken in this investigation were assumed to be representative of the soil water content at the mid-depth of the probe (i.e. 30 mm from the surface of the sample).

The sensor outputs a voltage that is correlated to the soil bulk dielectric permittivity ε by the following relationship:

$$\sqrt{\varepsilon} = 1.07 + 6.4 \cdot V - 6.4 \cdot V^2 + 4.7 \cdot V^3 \quad (6)$$

where V is the output voltage of the probe (Gaskin and Miller, 1996; Delta-T Devices Ltd., 1999). To convert the dielectric permittivity measurement to the soil water content the following relationship is suggested by the manufacturer:

$$\theta = \frac{\sqrt{\varepsilon} - a_0}{a_1} \quad (7)$$

where a_0 and a_1 are soil specific calibration parameters.

To confirm the accuracy of the relationship in Eq. (6), the dielectric constant of some common laboratory solvents (Acetone, Acetic Acid and Ethanol) was measured and checked against values quoted by Budevsky (1979), yielding an average percentage discrepancy of approximately ±1.2%, which was deemed acceptable.

Soil specific calibration of parameters a_0 and a_1 was then conducted on silica sands compacted into a mould of 150 mm height and 100 mm diameter. Compaction was achieved in three layers using a 250 g sliding hammer dropped from a height of 300 mm, with fifteen blows being applied per layer. Four target soil water contents in the range of 0–0.35 were tested to represent dry, damp, wet and saturated samples in both fine sand and coarse sand with grain size ranges of 0.075–0.2 mm and 0.4–0.6 mm respectively. After compaction of the sample the ThetaProbe was inserted and measurements taken for a period of 10 min, from which the time averaged root dielectric value was calculated using Eq. (6). Following this the soil water content of each sample was derived experimentally. Fig. 2 shows a plot of the measured root dielectric permittivity of the fine and coarse silica sand with respect to the measured volumetric water content showing that soil dielectric permittivity was not significantly grain size dependent. The calibration parameters a_0 and a_1 were determined using the method of least squares, yielding values of 1.492 and 9.743 respectively. The average discrepancy of the calibration function from the measured soil water content was ±0.03, which is less than the capability of the device as quoted by the manufacturer and thus deemed acceptable.

3.2.3. High air entry filter preparation

A simple high air entry filter was created using uniform silt with an estimated air-entry suction of approximately 20–30 kPa. The filter allows the transmission of water relatively rapidly at low applied suctions (0–15 kPa) but not air, thus allowing hydraulic suction to be maintained at the base of the sample.

The silt filter has two critical advantages in comparison to commercial high air-entry porous ceramics. It provides adequate air-entry suction for sand whilst ensuring higher hydraulic conductivity and subsequently shorter equalisation periods than for example, a commercial 100 kPa air-entry suction ceramic. Additionally, it ensures proper contact with the sand and eliminates possible wall effects (large pores at the interface between a flat surface and a granular material) that could prevent suction being transmitted to the sample.

To construct the filter, first, a woven mesh was placed in the base of the test chamber, which was covered by a paper filter. Liquefied silt slurry was then poured on top of the filter paper and allowed to settle under gravity, generating a targeted 10 mm depth of filter. Excess water was then drained from the base, with clear water indicating a successful filter and cloudy water indicating failure. Following successful generation of the filter a test suction of 17 kPa was applied (which was greater than the target maximum suction of 15 kPa), whilst allowing complete drainage of the cylindrical cell and consolidation of the filter without filter desaturation. This exposed the filter to air, thus testing the ability of the filter to maintain hydraulic suction at the base of the sample. Before use each of the filters was tested in this manner.

3.2.4. Experimental procedure

Following creation of a successful air entry filter oven dried fine silica sand was rained into the cell, to attain a sample height of 150 mm with uniform density. The ThetaProbe was then placed into the centre of the sample, with an accompanying latex cover being used to isolate the sample from the atmosphere, thus minimising evaporation of pore water from the sample to the atmosphere. The cell was connected to the hydraulic reservoir using transparent plastic tubing, with an air trap at the point of lowest pressure in the system.

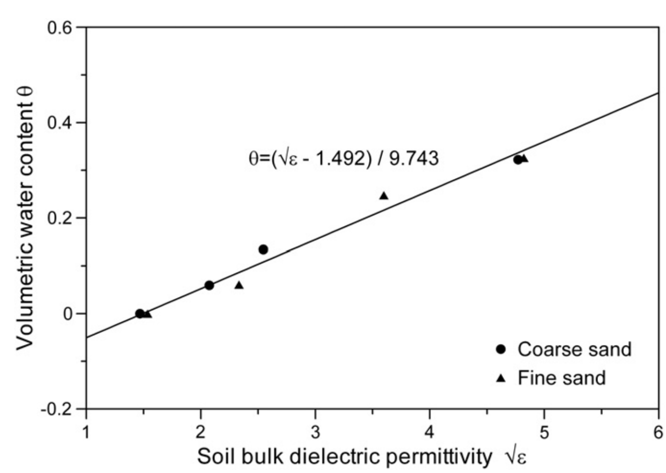

Fig. 2. Calibration of parameters a_0 and a_1 for fine and coarse grained silica sands.

Please cite this article as: Stanier, S.A., Tarantino, A., An approach for predicting the stability of vertical cuts in cohesionless soils above the water table, Engineering Geology (2013), http://dx.doi.org/10.1016/j.enggeo.2013.03.012

Upon assembly of the apparatus, the water reservoir was raised above the surface of the sand in the cylindrical cell to commence saturation, which was achieved when the water table was observed to be above the surface of the sand and the ThetaProbe was indicating a constant measurement.

After saturation of the sample, the drying phase was initiated by lowering the water reservoir in increments followed by the wetting phase by raising the water reservoir. This allowed the investigation of the hysteretic hydro-mechanical properties of the soil.

3.2.5. Experimental results

Fig. 3 presents the change in soil volumetric water content (θ) with respect to time in hours, with the final measurement points used to define the soil water retention drying and wetting curves indicated. A change in sample porosity was evident between the start and the end of the experiment. Fleuerau et al. (1993) observed in silty non-plastic soils that changes in void ratio were apparent during the drying phase but only significantly before the air entry suction was reached. If the same behaviour is assumed to be apparent here it is reasonable to assume all volumetric changes occurred before the air entry suction of the sand was reached. The porosity at all suctions exceeding the air-entry value could thus be assumed to be equal to the final porosity, which was measured at the end of the experiment.

After correction of the initial soil water content measurement based upon this assumption, the van Genuchten (1980) relationship describing soil water retention characteristics was fitted using the least squares method for both the drying and wetting water retention curves as illustrated in Fig. 4. The following equations were used to model the main drying curve and the scanning wetting curve respectively:

$$S_r = \left(\frac{1}{1+(\alpha_d s)^{n_d}}\right)^{m_d} \quad \text{(Main drying)} \tag{8}$$

$$S_r = S_{r0} + (1-S_{r0})\left(\frac{1}{1+(\alpha_w s)^{n_w}}\right)^{m_w} \quad \text{(Scanning wetting)}. \tag{9}$$

The scanning wetting curve was modelled by setting a ‘residual’ degree of saturation S_{r0} greater than 0. Table 1 summarises the Van-Genuchten parameters fitted for both the drying and wetting paths.

The difference in parameters used to fit the Van-Genuchten relationship is evidence of the hysteretic behaviour of the silica sand investigated. Thus for a given suction, two distinct degrees of saturation could exist dependent upon whether the soil is in a drying or wetting cycle. Thus in relation to shear strength, if the shear strength of the sand is assumed to be a function of suction multiplied by degree of saturation, then the soil can exhibit two distinct shear strengths at the same suction, depending on whether the degree of saturation lies on the drying or wetting curve. This hypothesis was investigated by performing simple column collapse tests on samples on both the drying and wetting paths.

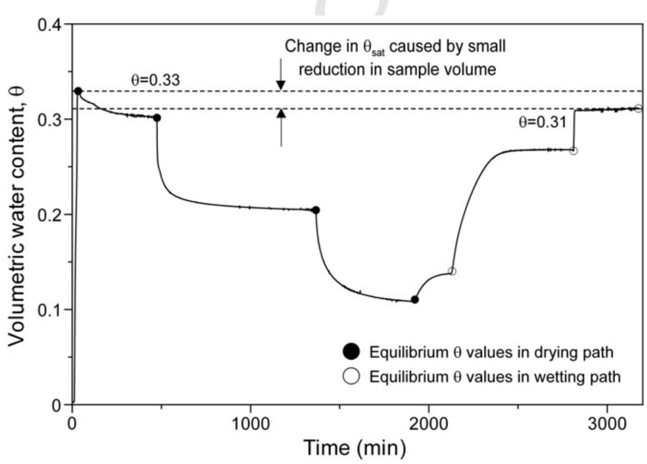

Fig. 3. Equalisation of hydraulic suction during water retention characteristic curve derivation experiment, performed on uniform fine sand.

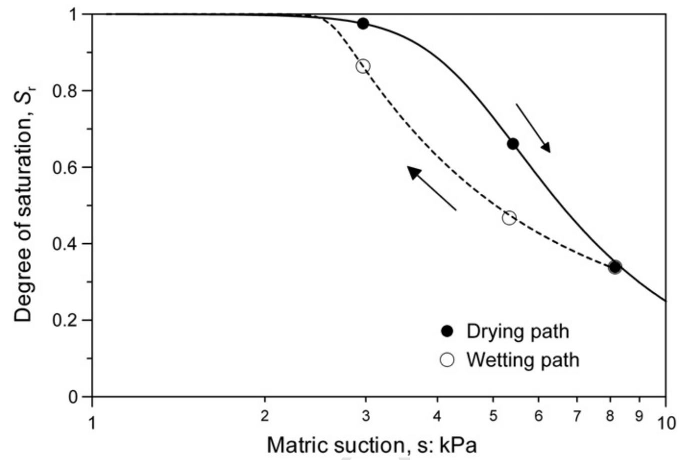

Fig. 4. Water retention curves for drying and wetting paths fitted using the Van-Genuchten relationship.

3.3. Column collapse tests

3.3.1. Apparatus

A 100 mm diameter triaxial base and split-form was used in place of the cylindrical cell to form the samples for the column collapse tests. A high air entry filter was created in the base of the split-form following the same method as previously described for the soil water retention experiment ~~(Figure 5)~~. Q4

(Figure 5) Change

3.3.2. Experimental procedure

Following testing of the air entry filter, oven-dried fine sand was rained into the split-form to create a sample of uniform density, with depth of 180 mm and diameter of 100 mm. Next the sample was saturated by raising the water reservoir to provide a small positive head potential at the surface of the sample. This was followed by either drying to a target applied suction or drying to an applied suction of 8.2 kPa, followed by wetting to a target applied suction at the base of the sample. Due to a ThetaProbe not being placed in-situ in the sample, to facilitate collapse testing on a virgin sample, it was not possible to observe constant soil-water content using the ThetaProbe in these experiments. As a result, a period of 24 h was allowed for equalisation of matric suction following the application of a suction increment either in drying or wetting. This was seen as a conservative estimate of the time required for equalisation of suctions within the sample according to the response observed in the water retention test.

After the allowed equalisation period the split-form was removed, revealing a cylindrical column of sand that could be loaded in compression to failure. Loading was facilitated using a triaxial loading

Table 1
Van-Genuchten parameters fitted for drying and wetting hydro-mechanical behaviours.

Main drying		Scanning wetting	
α_d	0.219	α_w	0.384
n_d	5.81	n_w	29.10
m_d	0.32	m_w	0.046
		S_{r0}	0.15

Please cite this article as: Stanier, S.A., Tarantino, A., An approach for predicting the stability of vertical cuts in cohesionless soils above the water table, Engineering Geology (2013), http://dx.doi.org/10.1016/j.enggeo.2013.03.012

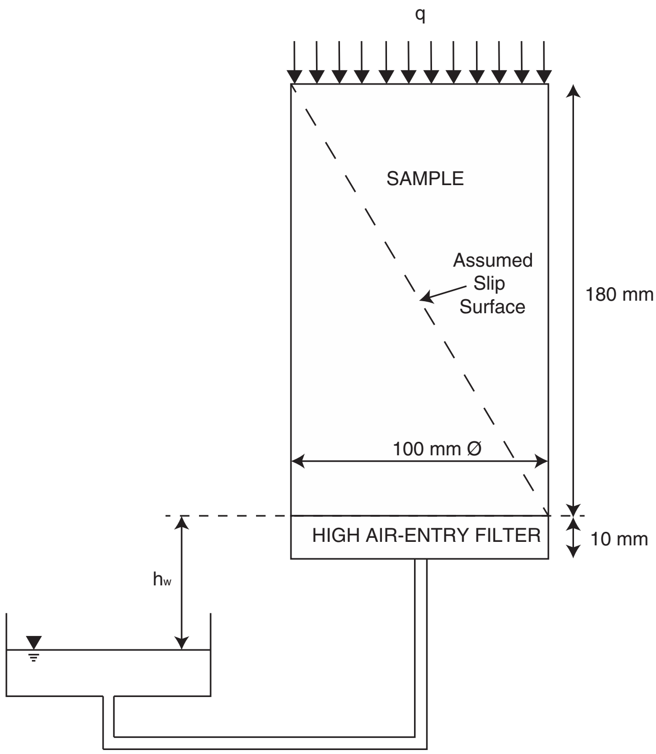

Fig. 5. Schematic of apparatus used to generate collapse in the sand sample.

cap and a plastic hopper, into which small ball bearings were placed until failure. The mass of the loading cap and ball bearings at failure allowed calculation of the failure boundary pressure for the sample.

3.3.3. Experimental results

Collapse boundary pressures are plotted against the suction applied at the base of the sample in Fig. 6. The results clearly show that there is a hysteretic effect and it will later be demonstrated that this is associated with the hysteresis of the water retention curve.

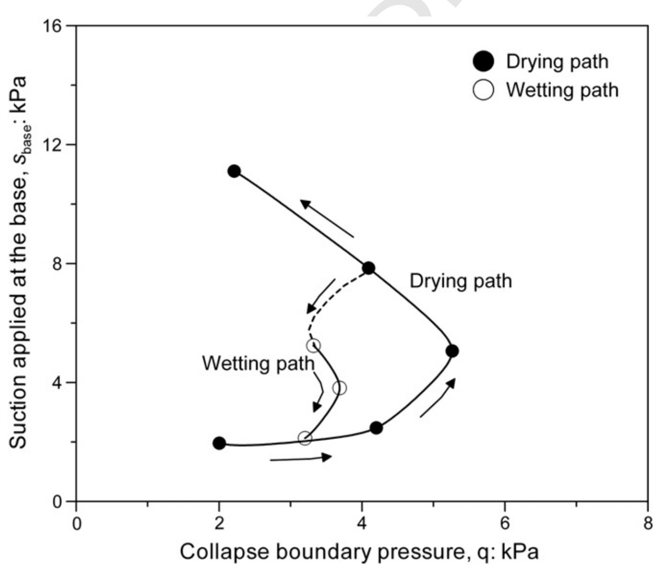

Fig. 6. Collapse boundary stresses measured on samples subjected to drying and wetting hydraulic paths.

3.4. Prediction of the upper and lower bounds of collapse pressure

3.4.1. Failure criterion

The following failure criterion was adopted for the sand according to Öberg and Sällfors (1997):

$$\tau = (\sigma + sS_r)\tan\phi'. \tag{10}$$

The internal angle of friction ϕ' of the fine sand was estimated in a very simple manner using a tilting slide mechanism. Sand was placed in a Perspex slide formed from three pieces of Perspex to make a slide 1 m long and 0.15 m wide with sides to contain the sand and a rough surface along the base. The sand was placed in a uniform thickness of approximately 30 mm depth. The slide was then tilted until movement of the sand was observed; indicating the angle of the slope of the slide had exceeded the angle of friction of the sand material. The slide was then tilted back toward horizontal until the movement of the sand subsided. At which point the angle of the slide was calculated using simple trigonometry; thus giving an estimate of $\phi' = 32°$ for the critical angle of friction for the sand material. This simple method was preferred to the more conventional direct shear or triaxial tests as the low stresses were more representative of those apparent in the experiments presented in the previous section.

3.4.2. Estimating degree of saturation

To model shear strength by Eq. (10), the degree of saturation S_r needs to be estimated as a function of suction. For the case where tests were performed along the draining path, the main drying curve given by Eq. (9) was used because points at any elevation in the sample all desaturated from a saturated state (State *0* in Fig. 7:

For the case where the sample was wetted after being partially dried by lowering the reservoir to H_w^* (see Figure 7), the scanning curve given by Eq. (10) was used. As points at different elevations in the sample had previously been dried to different degrees of saturation, they followed different scanning paths as illustrated in Fig. 7 (hydraulic paths 1–2). The scanning wetting curve was modelled by scaling the wetting curve using the parameter S_{r0}. It can be demonstrated that this parameter can be derived as follows:

$$S_{r0}(z) = \frac{\left(\frac{1}{1+[\alpha_d \cdot s^*(z)]^{n_d}}\right)^{m_d} - \left(\frac{1}{1+[\alpha_w \cdot s^*(z)]^{n_w}}\right)^{m_w}}{1-\left(\frac{1}{1+[\alpha_w \cdot s^*(z)]^{n_w}}\right)^{m_w}} \tag{11}$$

where $s^*(z)$ is the suction at the end of the drying process generated by the water level H_w^* as shown in Fig. 7.

3.4.3. Lower bound solution of collapse boundary pressure

To derive the lower bound solution, we assume the axial and radial directions to be principal stress directions. The axial and radial stress, σ_a and σ_r respectively, are therefore given by

$$\begin{aligned} &\sigma_r = 0 \\ &\sigma_a = q + \left[\int_0^z \gamma(z)dz\right] \cdot z \end{aligned} \tag{12}$$

where q is the applied pressure at the top of the sample, z is the depth from the sample top surface, and q is the unit weight. The latter is in turn a function of the degree of saturation:

$$\gamma = \gamma_s(1-n) + \gamma_w Sn \tag{13}$$

where γ_s and γ_w are the specific weights of the solids and water respectively $\gamma_s = 26.7$ kN/m^3 and $\gamma_w = 9.81$ kN/m^3) and n is the porosity ($n = 0.31$).

Please cite this article as: Stanier, S.A., Tarantino, A., An approach for predicting the stability of vertical cuts in cohesionless soils above the water table, Engineering Geology (2013), http://dx.doi.org/10.1016/j.enggeo.2013.03.012

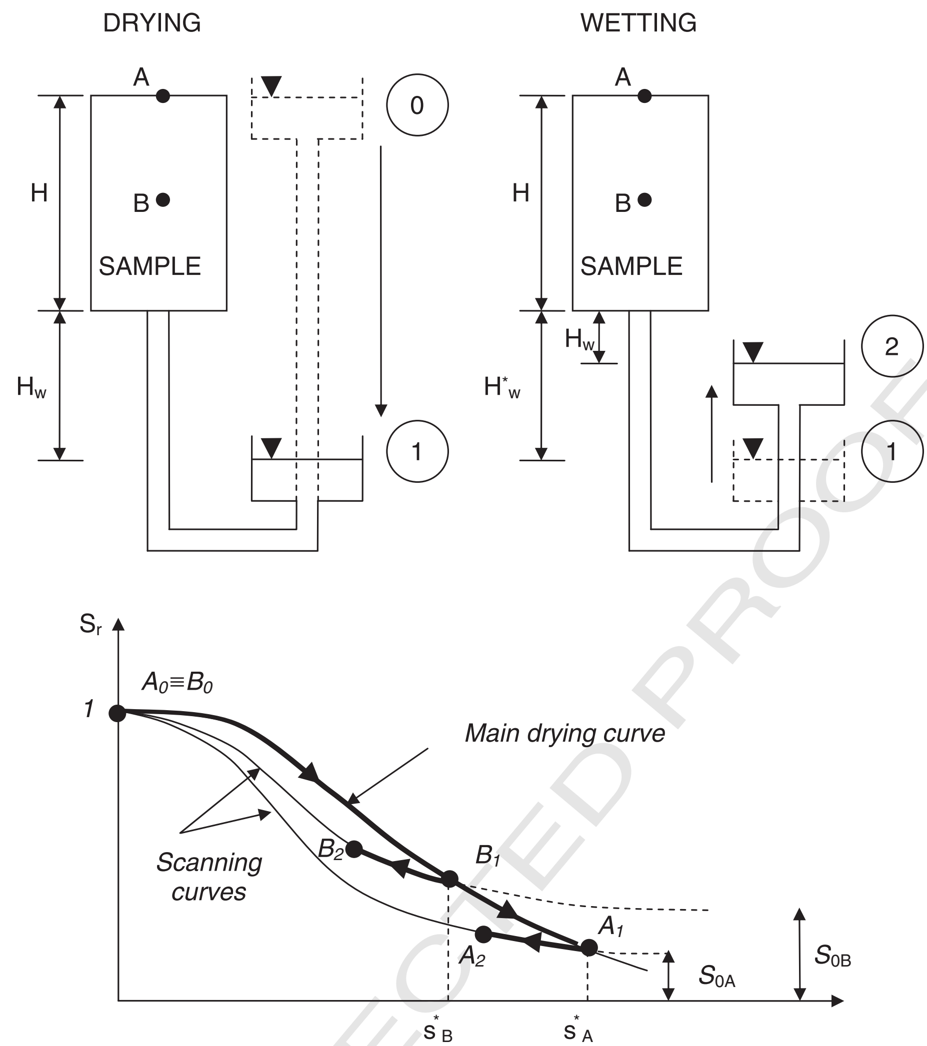

Fig. 7. Hydraulics paths followed at different elevations (e.g. *A* and *B*) in the samples during the drying path (0–1) and wetting path (1–2).

The lower bound solution for the collapse pressure q is obtained by imposing that the Mohr circle at the base of the sample is a tangent to the failure envelope in σ''–τ space as illustrated in Fig. 8:

$$q_l = \left(k_p - 1\right)\left[s(H)S_r(H)\right] - \int_0^H \gamma(z)dz \tag{14}$$

where k_p is the passive earth coefficient.

3.4.4. Upper bound solution of collapse boundary pressure

The upper bound solution was derived by considering a single block mechanism with a planar failure surface formed at an angle β to the vertical as illustrated in Fig. 9. It was found that the minimum upper bound value of the collapse pressure is obtained for the angle generating a failure surface that cuts the cylinder in two halves as shown in Fig. 9.

The upper bound collapse load is obtained by equating the external work associated with the pressure q and the self-weight W with the internal work done by shear and normal stresses along the failure surface:

$$\left(W + q\frac{\pi d^2}{4}\right)\delta\cos(\beta + \varphi') = \delta\sin\varphi' \int_L sS_r dL \tag{15}$$

where δ is the displacement of the block, d is the sample diameter, q is the pressure applied at the boundary, and W is the self-weight of the sliding bock. By rearranging this equation we obtain:

$$q_u = \frac{4}{\pi d^2}\left[\frac{\sin\varphi'}{\cos(\beta + \varphi')}\int_L sS_r dL - W\right] \tag{16}$$

with the failure stress q_u, the self-weight W and the integral $\int sS_r dL$ calculated numerically by subdividing the problem vertically into 100 discrete parts. Therefore when calculating the degree of saturation along a scanning wetting path, 100 different scanning curves were used which were described by the scaling parameter defined by Eq. (11).

3.5. Discussion

The lower and upper bound envelopes for the drying and wetting paths are shown in Fig. 10 together with the experimental results. The lower and upper bound solutions appear to bracket the experimental data showing that the theorems of bound plasticity can adequately capture the collapse behaviour even for partially saturated soils. Although simplistic, this, to the authors' knowledge, represents the first validation of limit analysis for partially saturated soils.

The lower and upper bound solutions were derived under two assumptions that might seem to be questionable at first glance: (i) an

Please cite this article as: Stanier, S.A., Tarantino, A., An approach for predicting the stability of vertical cuts in cohesionless soils above the water table, Engineering Geology (2013), http://dx.doi.org/10.1016/j.enggeo.2013.03.012

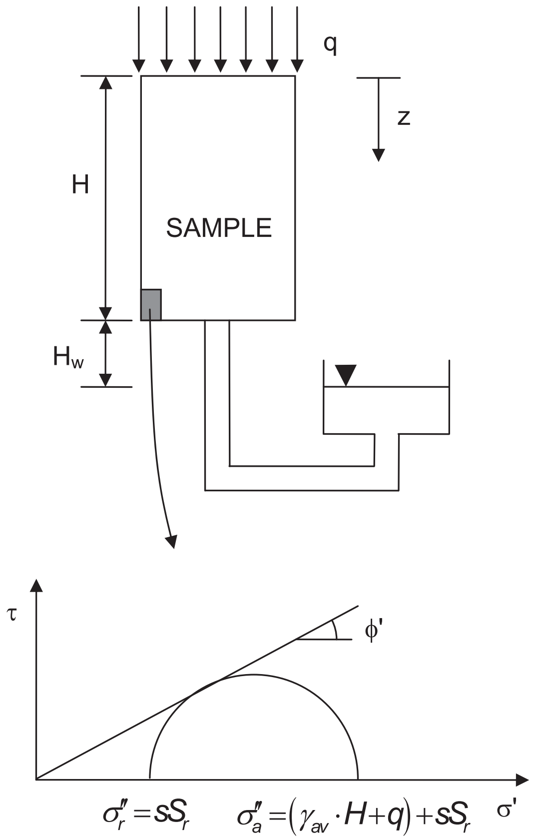

Fig. 8. State of stress to determine a lower bound collapse pressure using the lower bound theorem of plasticity.

associative flow, i.e. a dilatancy angle, $\psi = 32°$; and (ii) a friction angle equal to the critical (ultimate) friction angle, ϕ'_{crit}. The first assumption, although unrealistic, leads to an upper bound solution that coincides with the solution obtained by the limit equilibrium method, which is the simplest approach to understand and apply in geotechnical design. On the other hand, the adoption of the critical friction angle allows for a conservative estimate of the collapse load that tends to compensate for the overestimation associated with the associative flow.

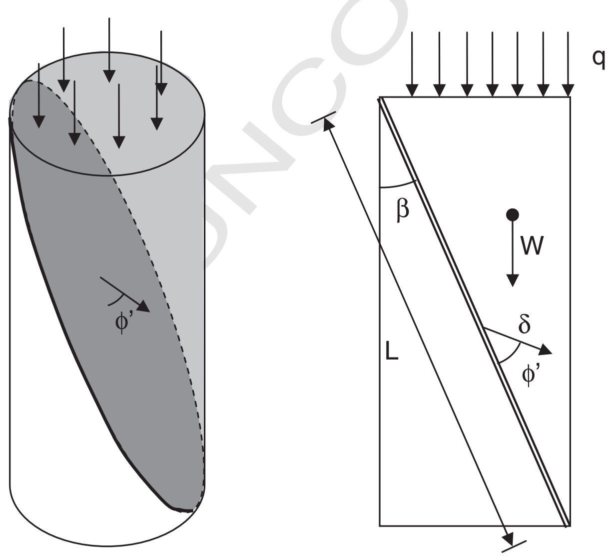

Fig. 9. Kinematic mechanism to determine an upper bound collapse pressure using the upper bound theorem of plasticity.

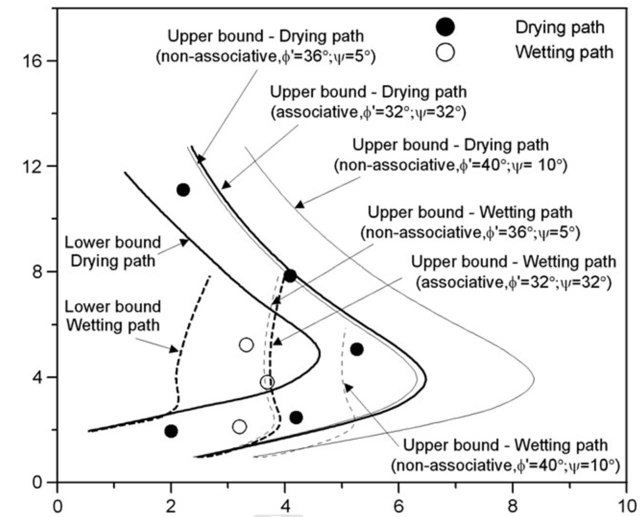

Fig. 10. Collapse boundary stresses predicted using the bound theorems of plasticity and comparison with experimental results.

This is demonstrated by a simple calculation of the upper bound collapse load using a non-associated flow rule. Bolton (1986) has demonstrated that sands tend to dilate even at relatively low relative densities and relatively high mean stresses. A non-zero dilatancy leads, in turn, to a peak friction angle that is greater than the critical state angle. Bolton proposed a widely used relationship between the peak friction angle, ϕ'_{peak}, the critical friction angle ϕ'_{crit}, and the dilatancy, ψ:

$$\phi'_{peak} - \phi'_{crit} = 0.8\psi. \tag{17}$$

As an example, for the sand tested in this programme ($\phi'_{crit} = 32°$), $\psi = 5°$ generates peak friction angle $\phi'_{peak} = 36°$ and $\psi = 10°$ generates peak friction angle $\phi'_{peak} = 40°$.

To estimate the upper bound load for soils with non-associated flow rules, Drescher and Detournay (1993) suggested using rigid block mechanisms with reduced discontinuity strength. This reduced strength is a function of the friction and dilatancy angle, ϕ'^{*} and follows the formula derived by Davis (1968):

$$\tan\phi'^{*} = \frac{\cos\psi \cdot \sin\phi'}{1 - \sin\psi \cdot \sin\phi'} \tag{18}$$

where ϕ' and ψ are the friction and dilation angles respectively.

To appreciate the role of dilatancy, the upper bound collapse load was calculated using Eq. (18) for two values of dilatancy angles, $\psi = 5°$ and $\psi = 10°$, and corresponding values of peak friction angle $\phi'_{peak} = 36°$ and $\phi'_{peak} = 40°$ respectively. The results from this analysis are shown in Fig. 10 where it can be seen that the non-associative solution for a small value of the dilatancy angle ($\psi = 5°$) is very similar to the one obtained by assuming associative flow using the critical friction angle ($\phi'_{crit} = 32°$ and $\psi = 32°$) and the solution obtained for higher dilatancy angle ($\phi'_{peak} = 40°$ and $\psi = 10°$ in Figure 10) leads to a significant overestimation of the collapse load.

This demonstrates that the classical upper bound solution based on associative flow and friction angle equal to the critical one, widely used in geotechnical design even if disguised in the form of the limit equilibrium method, is acceptable for engineering purposes.

4. Case study: Pozzolan Quarry

A demonstration of the application of this approach is to consider the maximum unsupported vertical cut height in a cohesionless soil in the field. De Vita et al. (2008) described vertical cuts up to 15 m

Please cite this article as: Stanier, S.A., Tarantino, A., An approach for predicting the stability of vertical cuts in cohesionless soils above the water table, Engineering Geology (2013), http://dx.doi.org/10.1016/j.enggeo.2013.03.012

high in a pyroclastic Pozzolan deposit in a quarry in the Campi Flegrei area near Naples in Italy with a water table depth of a few tens of metres. The authors were successful in capturing the correct order of magnitude of the critical height but they used a rather simplistic approach that would be problematic to use in engineering practice. They estimated the contribution of suction to shear strength using a linear relationship (Fredlund et al., 1978), which is conceptually and experimentally incorrect since the failure envelope with respect to suction has been demonstrated to be markedly non-linear (Escario and Sáez, 1986). They also assumed a constant suction throughout the excavation, which is inadmissible since the suction varies with depth in a profile that depends on the groundwater table level and the hydraulic boundary condition at the ground surface.

By using the approach proposed and validated in the previous section, a more accurate estimate can be attained, which accounts for the depth of the water table and incorporates a more realistic shear strength criterion.

4.1. Mechanical and hydraulic characteristics of pozzolan deposit

The Pozzolan soil relevant to this case study was investigated by De Vita et al. (2008) by means of 7 samples labelled C1 to C7. The material is characterised by a field porosity n in the range 0.54–0.68 and a specific unit weight of the solids γ_s in the range of 23.6–25.2 kN/m^3 (average values of n of 0.63 and γ_s of 24.4 kN/m^3 are used in these calculations). The grain size distribution is characterised by a silt fraction in the range 0.32–0.50, a sand fraction in the range 0.45–0.52 and the absence of any clay fraction.

Water retention characteristics of the soil were investigated using a conventional tensiometer by De Vita et al. (2008). Water retention data is shown in Fig. 11a together with the van Genuchten function (Eq. (8)) which was optimised to fit the experimental data.

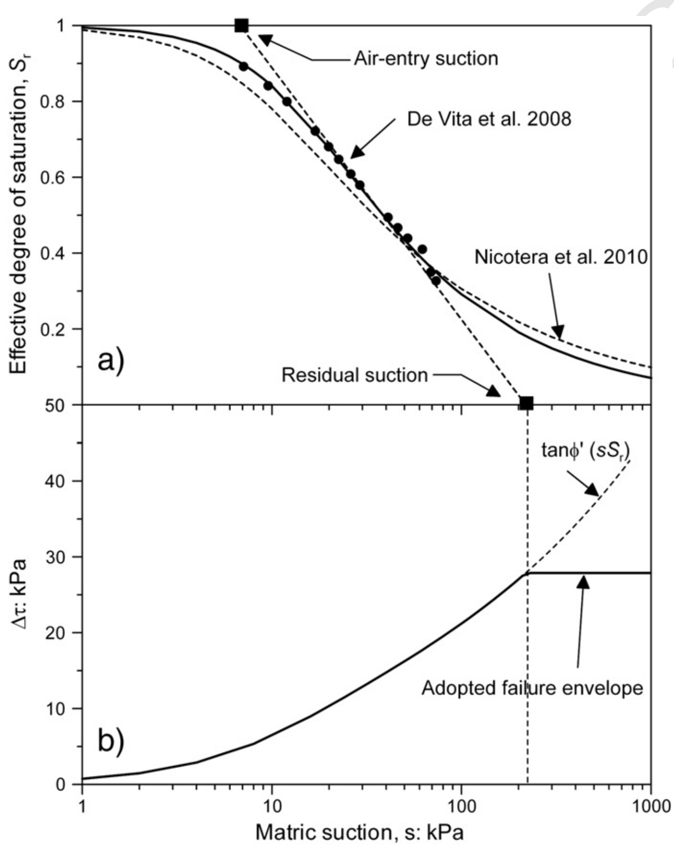

Fig. 11. Water retention curve (a) and shear strength criterion (b) for the pozzolanic soil in Campi Flegrei near Naples.

De Vita et al. (2008) did not carry out suction-controlled or suction-monitored tests on the pozzolan pyroclastic soils. However, shear strength of a very similar pyroclastic soil was investigated by Papa et al. (2008), whose water retention curve (Nicotera et al., 2010) is compared with the one obtained by De Vita et al. (2008) in Fig. 11a. Papa et al. (2008) observed that Eq. (4) models the experimental data in the range of suction 0–20 kPa very well with a friction angle $\phi' = 36.9°$.

When the shear strength criterion given by Eq. (4) is extrapolated at high suctions, it is found that the contribution of suction to shear strength, $\Delta\tau = s \cdot S_r \cdot \tan\phi'$, indefinitely increases with suction (Figure 11b), which is not intuitively acceptable. Eq. (4) is physically based on the effects of bulk water on the soil skeleton and can be anticipated to fail when pore-water is predominantly present in the form of menisci or adsorbed water as occurs at high suctions. As a first approximation, the residual suction shown in Fig. 11a may be assumed to delimit the range of menisci/bulk water and, hence, to limit the validity of Eq. (4). This assumption seems to be corroborated by Cattoni et al. (2007), demonstrating that Eq. (4) holds in the range of suctions bounded by the residual suction.

Accordingly, the contribution of suction to shear strength was assumed to become constant as the residual suction is exceeded as illustrated in Fig. 11b.

4.2. Stability of a vertical cut in pozzolan deposit

To derive an upper bound of the critical height H, the simplest kinematic mechanism was considered, which consisted of a single block with a planar slip surface inclined by the angle α as shown in shown in Fig. 12a. Considering that the unit weight γ of the soil is given by:

$$\gamma = (1-n)\gamma_s + n \cdot S_r \gamma_w \tag{19}$$

where n is the porosity, γ_s and γ_w are the specific unit weights of the solid particles and water respectively and S_r is the degree of saturation. The weight W of the block can be calculated as follows:

$$W = \gamma_s(1-n)\tan\alpha\frac{H^2}{2} + n\gamma_w \tan\alpha \int_H S_r(z)(H-z)dz \tag{20}$$

hence, the work done by the external forces W_e is equal to:

$$W_e = \left[\gamma_s(1-n)\tan\alpha\frac{H^2}{2} + n\gamma_w \tan\alpha \int_H S_r(z)(H-z)dz\right]\delta\cos(\alpha+\phi'). \tag{21}$$

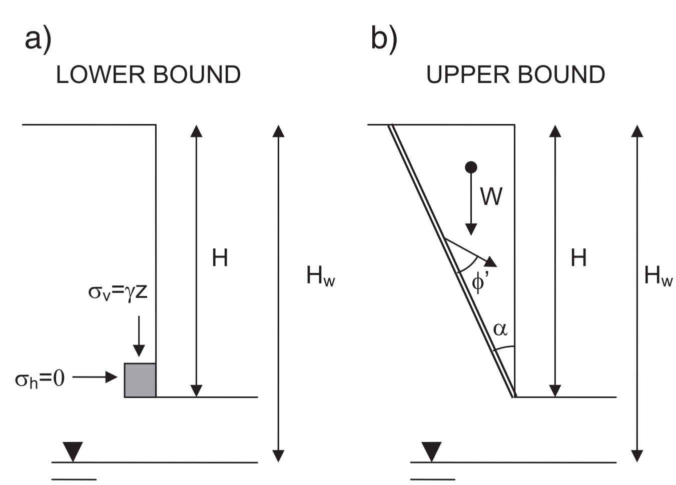

Fig. 12. (a) State of stress adopted to derive a lower bound solution and (b) kinematic mechanism to derive an upper bound solution for the critical height of a cut slope.

On the other hand, the internal energy dissipation W_i is given by:

$$W_i = \delta \frac{\sin\varphi'}{\cos\alpha} \int_H s(z) S_r(z) dz. \tag{22}$$

An upper bound solution for the critical height can then be obtained by equating W_e with W_i. It can then be demonstrated (see for example Stanier and Tarantino, 2010) that the minimum 'upper bound' value is obtained for:

$$\alpha = \frac{\pi}{4} - \frac{\phi'}{2}. \tag{23}$$

To derive a lower bound value for the critical height, we assume the vertical and horizontal directions to be principal directions of stress. Accordingly, the equilibrium stress state is given by:

$$\begin{cases} \sigma_z = \gamma z \\ \sigma_x = 0 \end{cases} \tag{24}$$

where σ_z and σ_x are the vertical and horizontal stresses. Based on the shear strength criterion given by Eq. (4) a lower bound can be obtained by imposing that the Mohr stress circle in the "$\sigma + sS_r, \tau$" plane relative to a point at the base of the excavation (Figure 12b) is a tangent to the failure envelope:

$$s(H) \cdot S_r(H) = k_a \{ [(1-n)\gamma_s + n \cdot S_r(H) \cdot \gamma_w] H + s(H) S_r(H) \} \tag{25}$$

where k_a is the active earth coefficient, s is the suction that is a function of H, and S_r is the degree of saturation that is in turn a function of suction s.

The lower and upper bound solutions obtained by assuming a hydrostatic suction profile are plotted in Fig. 13 as a function of the depth H_w of the water table. As expected, the critical height increases with the depth of the groundwater table, although the effect becomes less and less important at large values of the groundwater table depth. Fig. 13 shows that the calculated critical height is significant in this cohesionless material and this is in general agreement with field observations (see De Vita et al., 2008).

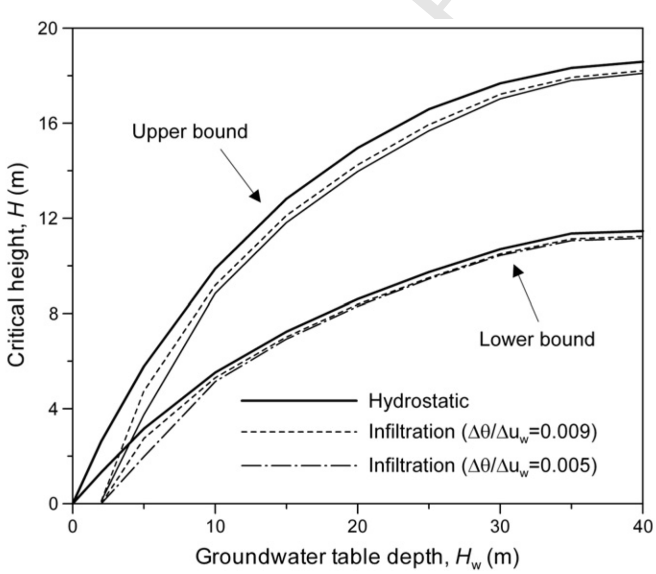

Fig. 13. Upper and lower bound solutions of critical height in pozzolan pyroclastic soil as a function of groundwater table depth assuming an hydrostatic suction profile and suction profiles generated by ponded infiltration.

4.3. Effect of rainfall on suction profile

Stability of vertical cuts in cohesionless soils has been demonstrated to rely on matric suction. However, its effect could partially or totally vanish when rainwater infiltrates at the ground surface. For engineering purposes, it becomes crucial to assess the potential impact of rainfall on matric suction and, hence, on vertical cut stability. A very simple method that allows preliminary assessment of this risk of vertical cut collapse is proposed here that is based upon solutions available in classical geotechnical textbooks focusing on saturated soils. The principal advantage of the method is that it can be used by practitioners lacking specific expertise in modelling water flow in unsaturated soils above the water table.

As a simplification the water flow equation may be linearised by assuming that hydraulic conductivity is constant and the water retention curve is linear. For conservatism the hydraulic conductivity is assumed to be equal to the saturated value ensuring a maximal infiltration rate and, hence, the highest reduction in suction and shear strength. Under these circumstances the water flow equation becomes (Tarantino et al., 2010):

$$\left(\frac{k_{sat}}{\gamma_w \frac{\Delta\theta}{\Delta u_w}} \right) \frac{\partial^2 u_w}{\partial x^2} = \frac{\partial u_w}{\partial t} \tag{26}$$

where u_w is the pore-water pressure, t is the time, z is the vertical coordinate, k_{sat} is the saturated hydraulic conductivity, γ_w is the unit weight of water, and $\Delta\theta/\Delta u_w$ is the slope of the linearised water retention curve. The water retention curve is highly non-linear and we suggest two possible linearisations in Fig. 14. It will be demonstrated later that these linearisations are essentially equivalent for the purpose of estimating suction profiles following rainfall.

Let us assume that the initial condition for pore-water pressure is hydrostatic and controlled by the groundwater table located at the depth H_w from the ground surface. This is a conservative assumption as evapotranspiration at the ground surface would generate suctions higher than those associated with hydrostatic conditions. To simulate infiltrating rainwater, the hydraulic boundary condition at the ground surface should be represented by an inward flux. For conservatism it is assumed that a pond immediately forms at the ground surface and that the hydraulic boundary condition is represented by zero pore-water pressure at the ground surface (i.e. ponded infiltration). This is the most conservative assumption as it returns the maximum possible infiltration and, hence, the highest reduction in suction. Therefore, the groundwater table and the ponded surface infiltration represent the hydraulic boundary conditions at the bottom and top of the flow domain.

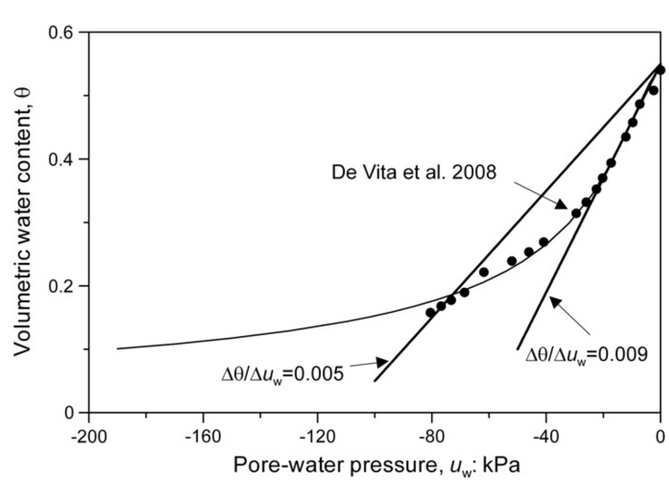

Fig. 14. Linearisation of the water retention curve for the pozzolan pyroclastic soil.

With these initial and boundary conditions, the problem reduces to the classical Terzaghi consolidation problem with triangular excess pore-water pressure and double-drainage. The solution of this problem is widely found in classical geotechnical textbooks, often in graphical form (e.g. Lambe and Whitman, 1969), and can therefore be exploited by engineers with no specific background in unsaturated soil mechanics. The solution is given by:

$$u(z,t)=\sum_{n=1}^{\infty}\frac{2u_0}{n\pi}\left\{1-\left(\frac{2H}{n\pi}\right)\sin(n\pi)\right\}\sin\frac{n\pi z}{2H}\exp\left(-\frac{n^2\pi^2T}{4}\right) \tag{27}$$

where u_0 is the initial excess pore-water pressure at the ground surface and T is the time factor given by:

$$T=\left(\frac{k_{sat}}{\gamma_w\frac{\Delta\theta}{\Delta u_w}}\right)\frac{1}{H^2}\cdot t \tag{28}$$

where H is the drainage length. By assuming $k_{sat}=7\cdot10^{-7}$ m/s (Nicotera et al., 2010), $\Delta\theta/\Delta u_w$ is equal to 0.005 or 0.009 (see Figure 14), and a rainfall duration of 2 days, we can derive the pore-water pressure profiles as shown in Fig. 15 for different water table depths H_w. It appears that rainfall only affects a shallow portion of the ground and its effects become less and less important as the depth of the groundwater table increases. If the lower and upper bound solutions are calculated by considering the pore-water pressure profiles after two days (ponded) infiltration, the values shown in Fig. 13 are obtained.

It appears that there is not a significant difference between the values derived under the assumption of hydrostatic pore-water pressure profile and either of the ponded surface infiltration solutions. Hence, the choice regarding the slope of the 'linearised' water retention curve is not overly critical. In conclusion therefore, rainfall does not seem to jeopardise slope stability, which compliments field observations (De Vita et al., 2008). It should be stressed again that the analysis of the effect of rainwater is definitively conservative since saturated hydraulic conductivity and ponded infiltration was considered.

5. Conclusions

An extension to the classical limit analysis has been proposed to allow assessment of the stability of excavations above the water table in cohesionless (granular) soils, which accounts for the beneficial effect of suction and partial saturation on shear strength. A modified shear strength criterion has been incorporated into the traditional bound theorems of plasticity approach using a relationship relating shear strength to the product of suction, s, and saturation ratio, S_r. This has facilitated analysis of the stability of vertical cuts in cohesionless soils above the water table.

To assess the validity of this extension, simple small-scale column collapse tests were performed using fine silica sand for which the water retention characteristics were derived using a negative-water column approach. The column collapse tests allowed assessment of the failure boundary pressure of the column for a given boundary suction applied to the base of the sample. Upper and lower bound solutions were derived for this boundary value problem, generating failure bounds that bracketed the experimental results reasonably well. To the authors' knowledge, this represents the first experimentally validated appraisal of the application of the bound theorems of plasticity to problems involving cohesionless soil above the water table.

The impact on practice of the findings of the laboratory validation tests was then explored using a case study, focussing on the vertical cut height observed in pyroclastic Pozzolan deposits near Naples, Italy. This problem has previously been addressed by De Vita et al. (2008) by introducing, however, several oversimplifications (constant matric suction within the excavation and linear 'unsaturated' failure envelope) that were removed in this paper. The upper and lower bounds for the safe vertical cut height were calculated accounting for varying suction, s, and saturation ratio, S_r, within the deposit and a non-linear failure envelope. These were solved using numerical integration and the calculated failure heights indicated good agreement with field observations of stable vertical cuts in pyroclastic Pozzolan deposits.

The impact of rainfall on infiltration and vertical cut stability was then explored. Simplifying the scenario of rainfall to a case with ponded infiltration and maximum (saturated) hydraulic conductivity, a conservative appraisal of vertical cut stability was generated using the classical Terzaghi consolidation solution for double drainage and a triangular excess pore pressure distribution. The impact of 2 days of constant rainfall causing ponded infiltration has been demonstrated to minimally impact upon the vertical cut stability in Pozzolan soil. This would explain the long-term stability of the large vertical cuts (tens of metres) observed in Pozzolan deposits in the field (De Vita et al., 2008).

The findings of this paper present and validate an approach to assessing the stability of vertical cuts in cohesionless soils that are based principally upon methods taught in most undergraduate Civil Engineering courses and that require little specialist knowledge. Hence, it is envisaged that these techniques may be used in the future by practising engineers, to rationalise the often unexplained non-zero vertical cut height observed in cohesionless soils above the water table, for which classical soil mechanics theory offers no rational explanation.

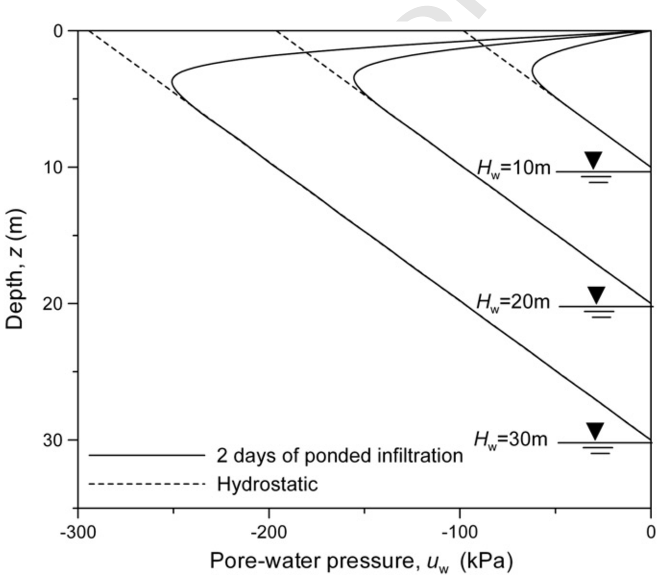

Fig. 15. Suction profiles after two days of ponded infiltration for water table depths of 10, 20, and 30 m.

References

Atkinson, J.H., 1981. Foundations and Slopes: An Introduction to Applications of Critical State Soil Mechanics. McGraw-Hill, London.
Bolton, M.D., 1986. The strength and dilatancy of sands. Geotechnique 36 (1), p65–p78.
Budevsky, O., 1979. Foundations of chemical analysis. British Library Cataloguing in Publication Data.Ellis Horwood Ltd. Publishers0-85312-113-3.
Chen, W.F., 2007. Limit Analysis and Soil Plasticity. J. Ross Publishing 638.
Davis, E.H., 1968. Theories of plasticity and failure of soil masses. In: Lee, I.K. (Ed.), Soil Mechanics Selected Topics. Elsevier, New York (USA), pp. 341–354.
De Vita, P., Angrisani, A.C., Di Clemente, E., 2008. Engineering geological properties of the phlegraean pozzolan soil (Campania region, Italy) and effect of the suction on the stability of cut slopes. Italian Journal of Engineering Geology and Environment 2, 5–22.
Delta-T Devices Ltd., 1999. ThetaProbe user manual. Available at http://www.delta-t.co.uk.
Drescher, A., Detournay, E., 1993. Limit load in translational mechanisms for associative and non-associative materials. Geotechnique 43 (3), 443–456.
Escario, V., Sáez, J., 1986. The shear strength of partly saturated soils. Geotechnique 36 (3), 453–456.
Fleuerau, J.M., Kheirbek-Saoud, S., Soemitro, R., Taibi, S., 1993. Behavior of clayey soils on drying–wetting paths. Canadian Geotechnical Journal 30, 287–296.

Please cite this article as: Stanier, S.A., Tarantino, A., An approach for predicting the stability of vertical cuts in cohesionless soils above the water table, Engineering Geology (2013), http://dx.doi.org/10.1016/j.enggeo.2013.03.012

Fredlund, D.G., Morgestern, N.R., Widger, R.A., 1978. The shear strength of unsaturated soils. Canadian Geotechnical Journal 13 (3), 313–321.

Gaskin, G.J., Miller, J.D., 1996. Measurement of soil water content using a simplified impedance measuring technique. Journal of Agricultural Engineering 63, 153–160.

Lambe, T.W., Whitman, R.V., 1969. Soil Mechanics. John Wiley & Sons.

Langendoen, E.J., Simon, A., Klimetz, L., Bankhead, N., Ursic, M.E., 2012. Quantifying sediment loadings from streambank erosion in selected agricultural watersheds draining to Lake Champlain. US Department of Agriculture – Agricultural Research Service, Technical Report No. 72.

Nardi, L., Rinaldi, M., Solari, L., 2012. An experimental investigation on mass failures occurring in a riverbank composed of sandy gravel. Geomorphology 163–164, 56–69.

Nicotera, M.V., Papa, R., Urciuoli, G., 2010. An experimental technique for determining the hydraulic properties of unsaturated pyroclastic soils. Geotechnical Testing Journal 33 (4). http://dx.doi.org/10.1520/GTJ102769.

Öberg, A.L., Sällfors, G., 1997. Determination of shear strength parameters of unsaturated silts and sands based on the water retention curve. Geotechnical Testing Journal 20 (1), 40–48 (March 1997).

Rinaldi, M., Casagli, N., 1999. Stability of streambanks formed in partially saturated soils and effects of negative pore water pressures: the Sieve River (Italy). Geomorphology 26, 253–277.

Rinaldi, M., Casagli, N., Dapporto, S., Gargini, A., 2004. Monitoring and modelling of pore water pressure changes and riverbank stability during flow events. Earth Surface Processes and Landforms 29, 237–254.

Romero, E., Vaunat, J., 2000. Retention curves in deformable clays. In: Tarantino, A., Mancuso, C. (Eds.), Experimental Evidence and Theoretical Approaches in Unsaturated Soils. A.A. Balkema, Rotterdam, pp. 91–106.

Simon, A., Curini, A., Darby, S.E., Langendoen, E.J., 2000. Bank and near-bank processes in an incised channel. Geomorphology 35, 193–217.

CRC Press

Change

Stanier, S., Tarantino, A., 2010. Active earth force in 'cohesionless' unsaturated soils using bound theorems of plasticity. In: Alonso, E.E., Gens, A. (Eds.), Proc. 5th Int. Conf. on Unsaturated Soils: vol. 2, vol. 2, pp. 1081–1086 (Barcelona, Spain, 6-8 September 2010). **Q8**

Tarantino, A., 2007. A possible critical state framework for unsaturated compacted soils. Geotechnique 57 (4), 385–389.

Tarantino, A., El Mountassir, G., in press. Making unsaturated soil mechanics accessible for engineers: preliminary hydraulic-mechanical characterisation & stability assessment. Engineering Geology. **Q9**

Tarantino, A., Tombolato, S., 2005. Coupling of hydraulic and mechanical behaviour in unsaturated compacted clay. Geotechnique 55 (4), 307–317.

Tarantino, A., Sacchet, A., Dal Maschio, R., Francescon, F., 2010. A hydro-mechanical approach to model shrinkage of air-dried green bodies. Journal of the American Ceramic Society 93 (3), 662–670.

Tsidzi, K.E.N., 1997. An engineering geological approach to road cutting slope design in Ghana. Geotechnical and Geological Engineering 15 (1), 31–45.

van Genuchten, M.T., 1980. A closed form equation for predicting the hydraulic conductivity of unsaturated soils. Soil Science Society of America Journal 44, 892–898.

Vanapalli, S.K., Oh, W.T., 2012. Stability analysis of unsupported vertical trenches in unsaturated soils. GeoCongress 2012 State of the Art and Practice in Geotechnical Engineering Geotechnical Special Publication No. 225 Oakland, California, USA 25-29 March 2012 Stability, 4, pp. 2502–2511.

Whenham, V., De Vos, M., Legrand, C., Charlier, R., Maertens, J., Verbrugge, J.C., 2007. Influence of soil suction on trench stability. In: Schanz, T. (Ed.), Experimental unsaturated soil mechanics. Proceedings in Physics, vol. 112, Part VII. Springer, pp. 495–501.

Zandarín, María T., Oldecop, L.A., Rodríguez, R., Zabala, F., 2009. The role of capillary water in the stability of tailing dams. Engineering Geology 105, 108–118.

Papa R., Urciuoli G., Evangelista A. and Nicotera M.V. (2008). Mechanical properties of unsaturated pyroclastic soils affected by fast landslide phenomena. In Unsaturated Soils, Advances in Geo-Engineering, Proceedings of the 1st European Conference, E-UNSAT 2008, Durham, United Kingdom, D.G. Toll, C.E. Augarde, D. Gallipoli, and S.J. Wheeler (eds), Taylor & Francis, pages 917–923.

Cattoni, E., Cecconi, M. and Pane, V. (2007). "Geotechnical properties of an unsaturated pyroclastic soil from Roma". Bull Eng Geol Environ, vol. 66: 403–414.

Please cite this article as: Stanier, S.A., Tarantino, A., An approach for predicting the stability of vertical cuts in cohesionless soils above the water table, Engineering Geology (2013), http://dx.doi.org/10.1016/j.enggeo.2013.03.012